Micro-Model Experimental Study of Fracture Geometrical Effect on Breakthrough Time in Miscible Displacement Process

Kamari, Ehsan; Rashtchian, Davood*+
Faculty of Chemical and Petroleum Engineering, Sharif University of Technology, P.O. Box 11365-9465 Tehran, I.R. IRAN

Shadizadeh, Sayed Reza
Department of Petroleum Engineering, Abadan Faculty of Petroleum Engineering, Petroleum University of Technology, Abadan I.R. IRAN

ABSTRACT: *The miscible displacement process appears to be an increasingly feasible method for the extraction of oil from depleted reservoirs. However, there is a lack of fundamental understanding of how fracture geometrical characteristics impact the oil recovery efficiency in this type of enhanced oil recovery technique. In this work, a series of experimental tests were conducted whereby the n-Heptane as a solvent displaced n-Decane in the glass micro-models having different fracture geometries. It has been observed that the breakthrough time is decreased with increasing the fractures' length. In contrast, breakthrough time is increased when increasing the fractures orientation angle related to flow direction. A correlation has been presented for the breakthrough time as a function of fracture length and its orientation.*

KEY WORDS: *Miscible displacement, Fracture geometrics, Glass micro-model, Breakthrough time.*

INTRODUCTION

Miscible recovery processes, in theory, are considered to be efficient because they eliminate capillary forces. In the absence of capillary pressure, no interface exists between miscible fluids of different composition. In solvent-based EOR techniques, several mechanisms affect the rate of the oil recovery, given that accessibility is provided: mass transfer and viscous forces cause the solvent to diffuse and/or disperse into the oil, reducing its viscosity.

Micro-models as the *Wilson* definition are transparent artificial models of porous media that can be used to simulate transport processes at the pore scale, and therefore are very attractive for this type of studies and give insight to the pore-scale interplay of various aspects of transport phenomena. It has been proven that microscopic visualization of the micro-model provides the opportunity to discover unrecognized processes and enhance the understanding of existing theories and assumptions [1].

Mattax & Kyte [2], made the first etched glass network, but this approach was significantly improved by *Davis & Jones* [3] by application of photo etching technique.

* To whom correspondence should be addressed.
+ E-mail: rashtchian@sharif.edu
1021-9986/11/3/1 7/$/2.70

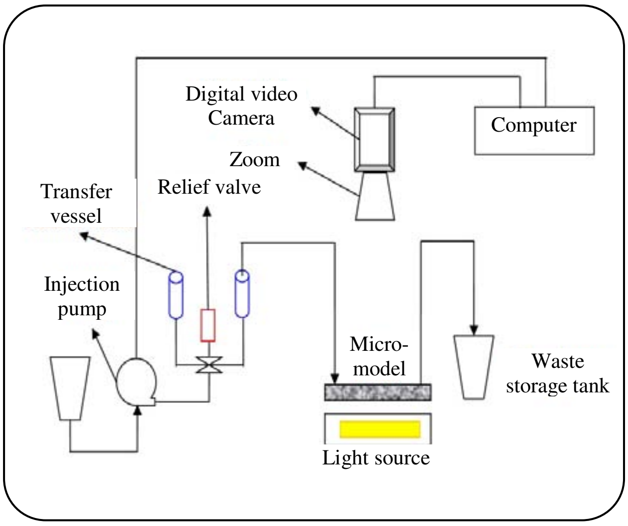

Fig. 1: Schematic diagram of experiment setup.

Micro-models are mostly fabricated by etching the desired pore network pattern on two plates of mirror glass that are then fused together. Using this method, highly intricate and detailed patterns can be etched with the dimensions of the pores and throats as low as a few microns. The models are provided with an inlet and an outlet at the two ends. The details of the models' production procedure are given elsewhere [4].

Almost all researchers have used micro-models, which have proven to be useful for studying a variety of oil recovery processes, and to obtain a better understanding of transport mechanisms during miscible/ immiscible displacements such as water flooding [5], gels for conformance control [6], miscible and immiscible displacements [7-13], surfactant floods [14,15], foamy oil flow [16], microbial EOR [17], and solution gas drive [18-21].

Micro-models have also been used to study specific aspects relating to flow in porous media, such as wettability [22-24], capillary pressure [25,26], asphaltene deposition [27], mass transfer [28,29], interfacial tension[30], heterogeneity[31], scaling[32], multiple contact miscibility [31,33], gravity drainage [34], imbibition and drainage [35,36], and breakthrough time in immiscible displacement process [37].

In this work, a series of experimental tests were conducted whereby the n-Heptane as a solvent displaced n-Decane in a glass micro-models having different fracture geometries to investigate the effect of single fracture geometrical characteristics (length and orientation) on the breakthrough time during miscible displacement process. This paper presents an experimental correlation to calculate breakthrough time as a function of fracture characteristics.

EXPERIMENTAL SECTION

This section presents micro-model apparatus, glass micro-model patterns, and experimental procedure.

Micro-model apparatus

The schematic diagram of the experimental setup is shown in Fig. 1. The micro-model setup is composed of: (1) a micro-model holder which is placed on a platform; (2) a camera which is equipped with a video recording system; (3) a precise pressure transducer; (4) a precise low rate pump which is used to control the flow rate of fluids through the micro-model. A high-accuracy, low-rate pump is used to control the flow rate of fluids through the micro-model. The pump is used to inject working fluid, depending on the request, from a low of 1.0×10^{-4} cm^3/min to a maximum 15 cm^3/min in the range.

Cleaning is accomplished by flushing solvent through the micro-model using another pump. This washing pump includes three containers for cleaning fluids (distilled water, acetone and toluene). In all micro-model experiments, the majority of data acquisition was achieved by visual observation. It was important to use high-definition optical equipment for image capturing and analyzing. A computer-controlled linear drive system was equipped by a magnifying video camera to be positioned automatically at any part of the micro-model and sequentially or continuously sweep the micro-model for video recording. The camera was capable of working at a magnitude of up to 200 times while running an experiment.

Glass micro-model patterns

Conventional software was used for designing different homogeneous and fractured patterns. These micro-models were constructed based on laser etched method. The homogeneous etched glass micro-model used in this work was a homogeneous sandstone representation of porous media, in which all pores and throats pervaded uniformly in space. Pores' sizes were in the range of 700 to 1200 micrometers and throats were in the range of 100 to 170 micrometers. Patterns with different fractured length and orientation were etched onto the surface of a glass plate. A second, optically flat glass plate was then placed over the first, covering the etched pattern and creating an enclosed pore space. This second plate (the cover plate) had an inlet and outlet hole drilled

Table 1: Physical and hydraulic properties of fractured micro-model patterns.

Properties	Patterns
Dimensions (cm×cm)	12×6
Pore diameter (µm)	700-1200
Throat Diameter (µm)	100-170
Fracture Width (µm)	1000
Matrix Porosity (%)	25.3
Matrix Permeability (Darcy)	0.863

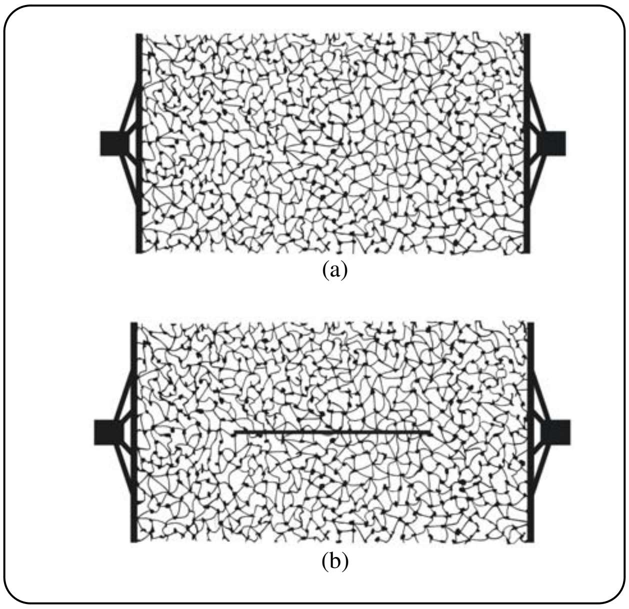

Fig. 2: Pattern of glass micro-models a) Homogeneous pattern b) Fractured pattern.

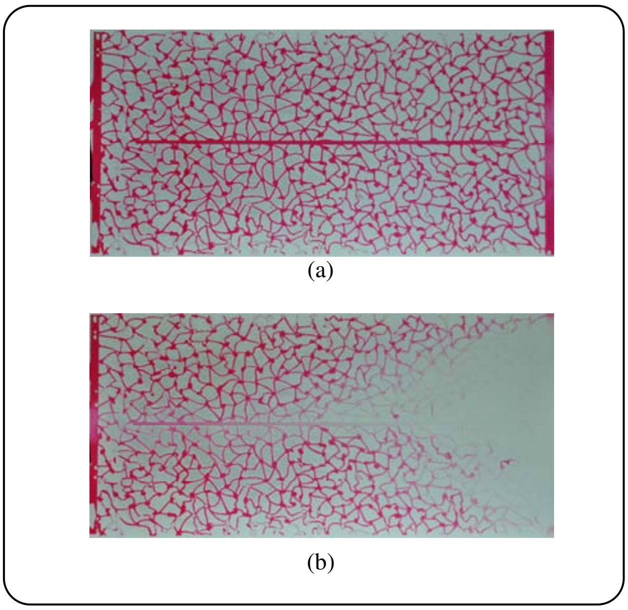

Fig. 3: Pattern of glass micro-models for L_{FD}=0.833 and θ=0° a) Before injection and b) At breakthrough time.

at both ends, allowing fluids to be displaced through the network of pores. This combination was placed into a special oven where temperature and heat flux controlled automatically. The heating process was started from ambient temperature to 724°C gradually and at the end of process the oven would be left to cool down slowly. This heating process, named the fussing process, was performed in order to completely seal the micro-models during the entire experiment. Length of micro-models was 12 cm and they had 6 cm width. In order to observe the effect of fracture orientation, seven fractured patterns had been generated with different inclinations 0, 15, 30, 45, 60, 75, and 90°. Also in order to observe the effect of fracture length, seven fractured patterns had been designed with different fracture lengths 3, 4, 5, 6, 8, 10, and 11cm. The schematic of previously mentioned patterns are shown in Fig. 2. The physical and hydraulic properties of different patterns are given in Table 1.

Experimental procedure

All of tests were carried out at a temperature of 21°C ± 0.5°C. In first step, before starting the experiments, the micro-model was cleaned with toluene/ethanol and de-ionized water to remove any extra material trapped inside the model. A low flow rate high-pressure pump was used for cleaning purposes. In second step, micro-models were saturated with n-C_{10}. In the last step, the solvent (n-C_7) was injected through the inlet port of the micro-model at a pre-selected flow rate. During the experiments a digital video camera captured images from the process and saved them in the computer every 30 seconds. Using of the captured images and data of injection pump, the breakthrough time was calculated.

Fig. 3 shows two image of the process. Experiments were repeated to check the reproducibility of the results.

RESULTS AND DISCUSSION

Effect of fracture length

To investigate the effect of fracture length on breakthrough time of miscible oil recovery displacement, micro-models with different fracture length of 3, 4, 5, 6, 8, 10, and 11cm with 0° fracture orientation to flow direction were used. The results are shown in Fig. 4. Fig. 4 shows breakthrough time as a function of injected pore volumes of solvent and L_{FD} (dimensionless fracture length) as length of fracture divided by injection length. Fig. 4 shows that the lengthier fracture in the micro-model causes the earlier breakthrough time.

Effect of fracture orientation

In order to observe the effect of fracture inclination (angle of fracture respect to flow direction), several micro-model patterns with different fracture's length and orientation to flow direction were used. The results of the miscible displacement tests conducted on the above micro-models are shown in Fig. 5. This figure shows that as the fracture orientation to flow direction was increased, later breakthrough time was observed. After breakthrough time, all the fractures were filled with the solvent and fractures acted as a solvent bank propagating solvent diffusion in oil within the matrix.

Correlation equation of the breakthrough time as a function of fracture length and its orientation

More than 40 experiments were conducted on different glass micro-model patterns with different fracture length and orientation. The results of experiment have similar trends for a specified fracture length with different orientation as shown in Fig. 6. Eq. (1) represents the trend of a specified fracture length with different fracture orientations.

$$t_{Bt} = (-5.5075L_{FD} + 0.8874)\times10^{-5}(90-\theta)^2 - (2.1510L_{FD} - 0.3466)\times10^{-3}(90-\theta) + 0.69 \quad (1)$$

Where: t_{Bt} is breakthrough time in pore volume of solvent injected, θ is orientation of fracture to flow direction in degree, and L_{FD} is dimensionless length (length of fracture divided by injection length).

Validity of the developed correlation equation

For validating Eq. (1), several new glass micro-model patters were used for conducting the same miscible

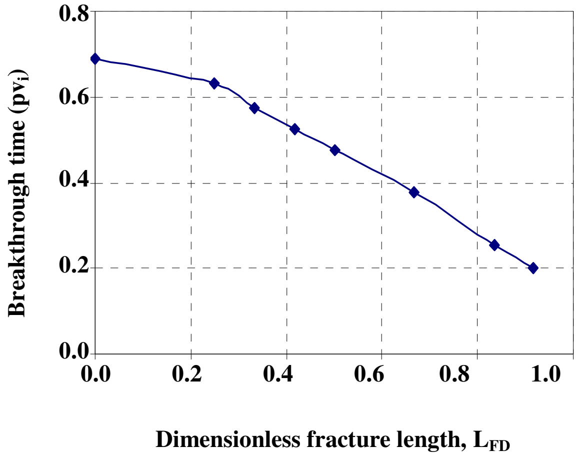

Fig. 4: Effect of fracture length on breakthrough time.

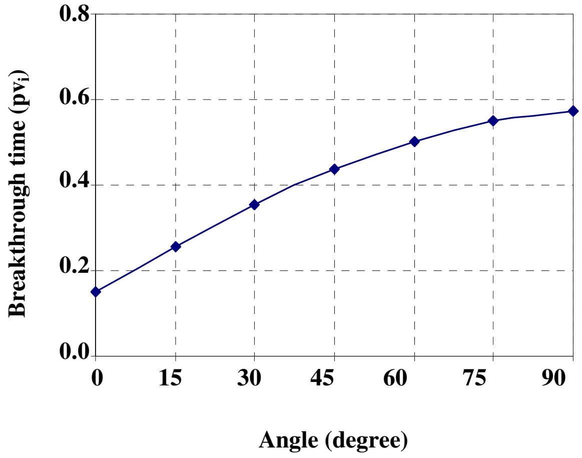

Fig. 5: Effect of fracture orientation for L_{FD}=0.5 on breakthrough time.

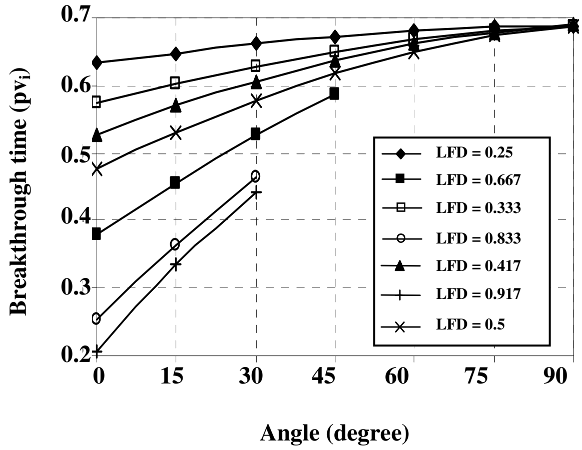

Fig. 6: Experimental breakthrough time values for different fracture length versus flow direction orientation angle.

Table 2: Physical and hydraulic properties of validating patterns.

Properties	Patterns
Dimensions (cm×cm)	12 × 6
Pore diameter (µm)	800
Throat Diameter (µm)	150
Fracture Width (µm)	1000
Matrix Porosity (%)	21.3
Matrix Permeability (Darcy)	0.985

Table 3: Comparison between experiment results and Equation (1).

Pattern No.	L_{FD}	Angle (degree)	Experiment Breakthrough Time (pv_i)	Correlation Breakthrough Time (pv_i)
1	0.333	15	0.611	0.609
2	0.417	45	0.628	0.637
3	0.500	20	0.551	0.548
4	0.667	30	0.517	0.525
5	0.833	30	0.459	0.470
6	0.917	70	0.635	0.641

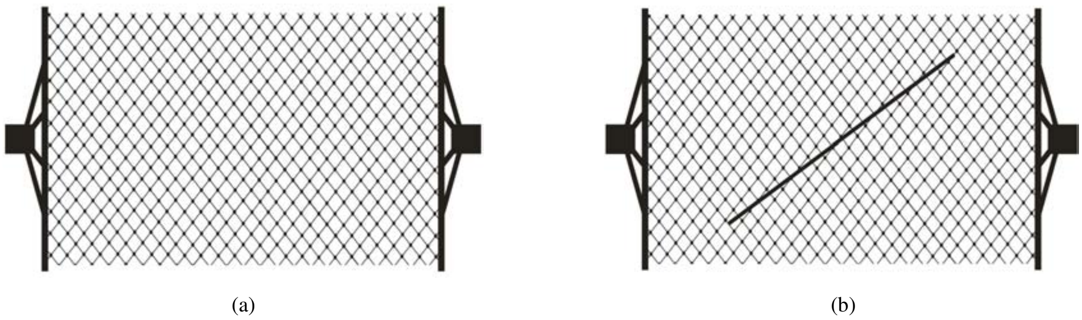

Fig. 7: Patterns of validating glass micro-model patterns a) homogeneous pattern b) fractured pattern with L_{FD}= 0.667 and θ=30°.

displacement tests. In these new glass micro-model patterns, porous media were different from previous patterns. Origin of these patterns is shown in Fig. 7. The physical and hydraulic properties of these new glass micro-model patterns are given in Table 2.

Fracture with different length and orientation was designed in these new micro-models and miscible displacement (displacing n-C_{10} by n-C_7) was conducted. The breakthrough time was calculated from image processing of these experiments was applied for validating Eq. (1). The results of these experiments were shown in Table 3. Graphical scheme of the developed correlation equation has been also shown in Fig. 8.

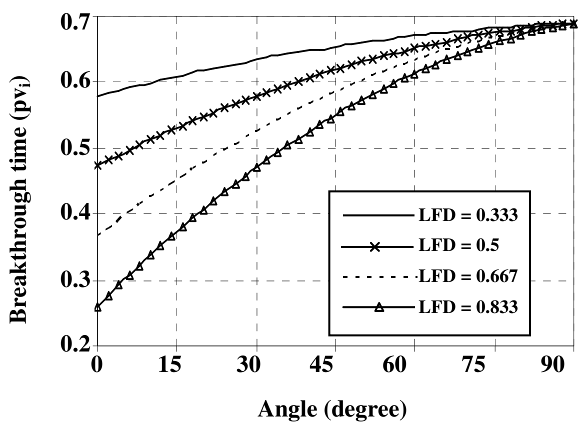

Fig. 8: Graphical scheme of Equation (1).

CONCLUSIONS

The following conclusions are made from this work:

1- Longer fracture length results earlier breakthrough time.

2- By increasing fracture orientation angle from 0° to 90° degrees, the breakthrough time increased.

3- The results showed there is an obvious relationship between breakthrough time and fracture geometrics (length and orientation angle), which was shown in Eq. (1).

Received : Jun. 11, 2010 ; Accepted : Aug. 1, 2011

REFERENCES

[1] Wilson J.L., "Visualization of Flow and Transport at the Pore Level," Proceedings of the Symposium on Transport and Reactive Processes in Aquifers, Dracos T.H., Stauffer F., Eds., Balkema, Rotterdam, Netherlands, pp. 19-36, 11-15 April (1994).

[2] Mattax C.C., Kyte J.R., Ever See a Water Flood, *Oil and Gas J.*, **59**, p. 115 (1961).

[3] Davis J.A., Jones S.C., Displacement Mechanisms of Residual Solutions, *J. Pet. Tech.*, **20**, p. 1415 (1968).

[4] McKellar M., Wardlaw N.C., A Method of Making Two Dimensional Glass Micromodels of Pore Systems, *J. Can. Pet. Technol.*, **21**, p. 1 (1982).

[5] Wang J., Dong M., Asghari K., Effect of Oil Viscosity on Heavy-Oil/Water Relative Permeability Curves, "SPE/DOE Symposium on Improved Oil Recovery", Tulsa, Oklahoma, 22-26 April(2006).

[6] Bai B., Lid Y., Coste J., Li L., Preformed Particle Gel for Conformance Control: Transport Mechanism through Porous Media, *SPE Reservoir Evaluation & Engineering*, **10**(2), p. 176 (2007).

[7] Sohrabi M., Henderson G.D., Tehrani D.H., Danesh A., Visualization of Oil Recovery by Water Alternating Gas (WAG) Injection Using High Pressure Micromodels - Oil-Wet & Mixed-Wet Systems, *SPE 71494*, Louisiana, 30 September-3 October (2001).

[8] Sohrabi M., Tehrani D.H., Danesh A., Henderrson G.D., Visualization of Oil Recovery by Water-Alternating-Gas Injection Using High-Pressure Micromodels, *SPE J.*, **9**(3), p. 290(2004).

[9] Sohrabi M., Danesh A., Tehrani D.H., Jamiolahmady M., Microscopic Mechanisms of Oil Recovery by Near-Miscible Gas Injection, *Transport in Porous Media*, **72**(3), p. 351 (2008).

[10] Danesh A., Krinis D., Henderson G.D., Peden J.M, Pore Level Visual Investigation of Miscible and Immiscible Displacements, *J. Pet. Sci. Eng.*, **2**(2-3), p.167 (1989).

[11] Touboul E., Lenormand R., Zarcone C., Immiscible Displacements in Porous Media: Testing Network Simulators by Micromodel Experiments, *SPE 16954*, "62nd Annual Technical Conference and Exhibition of SPE", Dallas, TX, 27-30 September (1987).

[12] Mahers E.G., Dawe R.A., Visualisation of Microscopic Displacement Processes Within Porous Media in EOR Capillary Pressure Effects, "3rd European Meeting on Improved Oil Recovery", Rome, **1**, pp. 40-58, 16- 18 April (1985).

[13] Chatzis I., Dullien F.A.L., Dynamic Immiscible Displacement Mechanisms in Pore Doublets: Theory versus Experiment, *J. Coll. Int. Science*, **91**(1), p. 199 (1983).

[14] Hornof V., Morrow N.R., Flow Visualization of the Effects of Interfacial Tension on Displacement, *SPE Reservoir Engineering*, **3**(1), p. 251 (1988).

[15] Paterson L., Hornof V., Neale G., Visualization of a Surfactant Flood of an Oil Saturated Porous Medium, *SPEJ*, **24**(3), p. 325 (1984).

[16] Bora R., Chakma A., Maini B.B., Experimental Investigation of Foamy Oil Flow Using a High Pressure Etched Glass Micromodel, "SPE Annual Technical Conference and Exhibition", Denver, Colorado, pp. 91-100, 5-8 October (2003).

[17] Soudmand-asli A., Ayatollahi S.S., Mohabatkar H., Zareie M., Shariatpanahi S.F., The in Situ Microbial Enhanced Oil Recovery in Fractured Porous Media, *J. Pet. Sci. Eng.*, **58**(1-2), p. 161 (2007).

[18] George D.S., Hayat O., Kovscek A.R., A Microvisual Study of Solution Gas-Drive Mechanisms in Viscous Oils, *J. Pet. Sci. Eng.*, **46**(1-2), p. 101 (2005).

[19] Grattoni C.A., Dawe R.A., Gas and Oil Production from Water flood Residual Oil: Effects of Wettability and Oil Spreading Characteristics, *J. Pet. Sci. Eng.*, **39**(3-4), p. 297 (2003).

[20] Lago M., Huerta M., Gomes R., Visualization Study During Depletion Experiments of Venezuelan Heavy Oils Using Glass Micromodels, *J. Can. Pet. Tech.*, **41**(1), p. 41 (2002).

[21] Danesh A., Peden J.M., Krinis D., Henderson G.D., Pore Level Visual Investigation of Oil Recovery by Solution Gas Drive and Gas Injection, *SPE 16956*, "62nd Annual Technical Conference and Exhibition of SPE", Dallas, Texas, 27-30 September (1987).

[22] Laroche C., Vizika O., Kalaydjian F., Wettability Heterogeneities in Gas Injection; Experiments and Modeling, *Petroleum Geoscience*, **5**(1), p. 65 (1999).

[23] Morrow N.R., Lim H.T., Ward J.S., Effect of Crude-Oil Induced Wettability Changes on Oil Recovery, *SPE Formation Evaluation*, **1**(1), p. 89 (1986).

[24] Romero-Zeron L., Kantzas A., The Effect of Wettability and Pore Geometry on Foamed-Gel-Blockage Performance, *SPE Res. Eval. & Eng.*, **10**(2), p. 150 (2007).

[25] Ghazanfari M.H., Khodabakhsh M., Kharrat R., Rashtchian D., Unsteady State Relative Permeability and Capillary Pressure Estimation of Porous Media, "CMWR - XVI International Conference", Copenhagen, Denmark, 18-22 June (2006).

[26] Ghazanfari M.H., Rashtchian D., Kharrat R., Voussughi S., Capillary Pressure Estimation of Porous Media Using Statistical Pore Size Function, *Chemical Engineering & Technology*, **30**(7), p. 862 (2007).

[27] Danesh A., Krinis D., Henderson G.D., Peden J.M., Asphaltene Deposition in Miscible Gas Flooding of Oil Reservoirs, *Chem. Eng. Res. Des.*, **66**, p. 339 (1988).

[28] Mahers E.G., Dawe R.A., The Role of Diffusion and Mass Transfer Phenomena in the Mobilization of Oil during Miscible Displacement, "European Symposium on Enhanced Oil Recovery," Paris, 279-288, 8-10 November (1982).

[29] Mahers E.G., Dawe R.A., Quantification of Diffusion inside Porous Media for EOR Processes by Micromodel and Holography, *SPE 12679*, "SPE/DOE Fourth Symposium on Enhanced Oil Recovery", Tulsa, Oklahoma USA, 16-18 April (1984).

[30] Mackay E.J., Henderson G.D., Tehrani D.H., Danesh A., The Importance of Interfacial Tension on Fluid Distribution During Depressurization, *SPE Reservoir Evaluation & Engineering*, **1**(5), p. 408 (1998).

[31] Bahralolom I.M., Bretz R.E., Orr Jr. F.M., Experimental Investigation of the Interaction of Phase Behavior with Microscopic Heterogeneity in a CO2 Flood, *SPE Reservoir Engineering*, **3**(2), p. 662 (1988).

[32] Ren X., Wu P., Qu Z., Shi C., Studying the Scaling Mechanism of Low-Permeability Reservoirs Using Visual Real-Sand Micromodel, "SPE International Oilfield Scale Symposium", Aberdeen, United Kingdom, 31 May-1 Jun (2006).

[33] Campbell B.T., Orr Jr. F.M., Flow Visualization for CO2/Crude Oil Displacements, *SPEJ*, **25**(5), p. 665 (1985).

[34] Ren W., Bentsen R.G., Cunha L.B., A Study of the Gravity Assisted Tertiary Gas Injection Processes, *J. Can. Pet. Tech.*, **44**(2), p. 26 (2005).

[35] Hatiboglu, C.U., Babadagli, T., Pore-Scale Studies of Spontaneous Imbibition into Oil-Saturated Porous media, *Phys. Review E*, **77**, 066311-11, (2008).

[36] Joekare Niasar V., Hassanzadeh S.M., Pyrak-Nolte L.J., Berentsen C., Simulating Drainage and Imbibition Experiments in a High-Porosity Micromodel Using an Unstructured Pore Network Model, *Water Resources Research*, **45**, W02430, 15 PP., (2009), doi:10.1029/2007WR006641.

[37] Kamari E., Shadizadeh S.R., Rashtchian D., Effect of Fracture Geometrics on Breakthrough Time in Immiscible Displacement Process through Strongly Oil WetFractured Porous Media: Experimental Investigation, Energy Sources, Part A: Recovery, Utilization, and Environmental Effects, accepted (2011).